Regulatory Role of Heparan Sulfate in Leptin Signaling

Naoko Nagai[1], Tatsumasa Shioiri[1], Sonoko Hatano[1], Nobuo Sugiura[1] and Hideto Watanabe[1]

[1]Institute for Molecular Science of Medicine, Aichi Medical University, 1-1 Yazakokarimata, Nagakute, Aichi, Japan

[1]Institute for Molecular Science of Medicine, Aichi Medical University
1-1 Yazakokarimata, Nagakute, Aichi, Japan

nnaoko@aichi-med-u.ac.jp (Naoko Nagai)
tatsumas@aichi-med-u.ac.jp (Tatsumasa Shioiri)
shatano@aichi-med-u.ac.jp (Sonoko Hatano)
nsugiura@aichi-med-u.ac.jp (Nobuo Sugiura)
wannabee@aichi-med-u.ac.jp (Hideto Watanabe)

Corresponding author: Naoko Nagai
[1]Institute for Molecular Science of Medicine, Aichi Medical University, 1-1 Yazakokarimata, Nagakute, Aichi, Japan
nnaoko@aichi-med-u.ac.jp

Abstract

Leptin, a hormone mainly secreted by adipocytes, has attracted significant attention since its discovery in 1994. Initially known for its role in appetite suppression and energy regulation, leptin is now recognized for its influence on various physiological processes, including immune response, bone formation, and reproduction. It exerts its effects by binding to receptors and initiating an intracellular signaling cascade. Heparan sulfate (HS) is known to regulate the intracellular signaling of various ligands. HS is present as the glycan portion of HSPGs on cell surfaces and in intercellular spaces, with diverse structures due to extensive sulfation and epimerization. Although HS chains on HSPGs are involved in many physiological processes, the detailed effects of HS chains on leptin signaling are not well understood.

This study examined the role of HS chains on HSPGs in leptin signaling using Neuro2A cells expressing the full-length leptin receptor (LepR). We showed that cell surface HS was essential for efficient leptin signaling. Enzymatic degradation of HS significantly reduced leptin-induced phosphorylation of downstream molecules, such as signal transducer and activator of transcription 3 and p44/p42 Mitogen-activated protein kinase. In addition, HS regulated LepR expression and internalization, as treatment with HS-degrading enzymes decreased cell surface LepR. HS was also found to exhibit a weak interaction with LepR. Enzymatic removal of HS enhanced the interaction between LepR and low-density lipoprotein receptor-related protein 1, suggesting that HS negatively regulates this interaction. In conclusion, HS plays a significant role in modulating LepR availability on the cell surface, thereby influencing leptin signaling. These findings provide new insights into the complex regulation of leptin signaling and highlight potential therapeutic targets for metabolic disorders and obesity.

Keywords: Leptin signaling, leptin receptor, heparan sulfate**,** endocytosis**,** low-density lipoprotein receptor-related protein 1

Abbreviations

The abbreviations used are as follows: CHase, chondroitinase; DAPI, 4',6-Diamidino-2-phenylindole Dihydrochloride *n*-Hydrate; ERK, Extracellular signal-related kinase; FACS, fluorescence-activated cell sorting; FGF, Fibroblast growth factor; HS, Heparan sulfate; HSPG, Heparan sulfate proteoglycan; HS6ST, Heparan sulfate 6-*O*-sulfotransferase; HSases, HS-degrading enzymes; JAK, Janus kinase; LepR, Leptin receptor; Lrp, Low-density lipoprotein receptor-related protein; MAPK, Mitogen-activated protein kinase; Ob-R, Ob receptor (LepR); PBS, phosphate-buffered saline; pERK1/2, phosphorylated ERK1/2; pSHP2, phosphorylated SHP2; pSTAT3, phosphorylated STAT3; SHP2, Src homolog domain-containing phosphatase 2; STAT, Signal transducer and activator of transcription.

1. Introduction

Leptin, a hormone primarily secreted by fat cells, has been extensively studied since its discovery in 1994 [1]. Beyond its well-known effects on body weight and appetite, leptin also influences various physiological processes, including immune response, bone formation, and the reproductive system, highlighting its multifaceted role in human biology[2–4]. Although leptin was initially identified as an appetite-suppressing hormone, recent studies have underscored its role in energy expenditure [5–7]. When leptin binds to its receptor on the surface of hypothalamic neurons, it triggers a cascade of intracellular signaling events that result in the transcriptional activation of genes like *Pro-opiomelanocortin* and *Suppressor of cytokine signaling 3*, while repressing genes such as *Neuropeptide Y* and *Agouti-related peptide* [8,9].

Among the six isoforms of the leptin receptor (LepR), only the longest variant possesses a cytoplasmic domain crucial for mediating physiological leptin signaling. Leptin signaling is intricate, involving diverse pathways, primarily the Janus kinase (JAK) / Signal transducer and activator of transcription (STAT) pathway. Upon leptin binding to LepR, JAK2 is activated, initiating subsequent phosphorylation of LepR at Tyr1138. This phosphorylation site serves as a docking site for the Src homology 2 domain of STAT3. After phosphorylation by JAK2, STAT3 translocates to the nucleus, where it regulates target genes as a transcription factor. [10]. In addition, leptin induces phosphorylation of Y985 in LepR, creating a binding site for Src homolog domain-containing phosphatase 2 (SHP2), which activates the Mitogen-activated Protein Kinase (MAPK) pathway [11]. Leptin also activates other regulatory proteins such as Insulin Receptor Substrate 1, Insulin Receptor Substrate 2, AMP-activated Protein Kinase, and the mammalian Target of Rapamycin [12].

LepR is a short-lived membrane protein that undergoes continuous endocytosis independent of ligands [13]. As a result, LepR is constantly internalized and recycled, regardless of the presence of leptin. Recent research has highlighted the critical role of LepR endocytosis in leptin signaling. Clusterin/Apolipoprotein J enhances leptin signaling by facilitating endocytosis mediated by low-density

lipoprotein receptor-related protein (Lrp) 2. This enhancement promotes leptin's appetite suppression and facilitates leptin-induced activation of hypothalamic STAT3 [14]. Blocking hypothalamic Lrp and its endocytosis disrupts leptin-induced anorexia and phosphorylation of hypothalamic STAT3. Thus, Lrp-mediated endocytosis of the leptin–LepR complex appears indispensable for the effective activation of STAT3 signaling by leptin [15]. Moreover, endospanin-1 and endospanin-2 act as negative regulators of cell surface expression of the longest LepR form and are involved in regulating membrane transport following LepR internalization through the endocytosis pathway [16]. These findings underscore the crucial role of LepR endocytosis in mediating leptin signaling that underlies appetite suppression in the brain.

Heparan Sulfate (HS) is a glycosaminoglycan chain that is covalently linked to serine residues in the protein core of Heparan Sulfate Proteoglycans (HSPGs), which are widely distributed on cell surfaces throughout the body [17,18]. These membrane-bound HSPGs play a crucial role in cell signaling and interactions. Comprising linear polysaccharides chains, HS consists of repeating disaccharide units of hexuronic acid and D-glucosamine residues that undergo various enzymatic modifications [19,20]. These include epimerization of glucuronic acids to iduronic acids, *N*-deacetylation and *N*-sulfation of *N*-acetylglucosamine, and addition of sulfate groups to the C6 and C2 positions of glucosamine residues. These modifications allow HS to participate in numerous signaling pathways by interacting with a diverse array of ligands and receptors [21,22]. Studies of genetic mutations in enzymes responsible for HS synthesis have revealed that alterations in HS structure can impact brain function [23–27]. In addition, HS-modifying enzymes such as Heparan sulfate 6-*O*-sulfotransferase 2 (HS6ST2) and an HS proteoglycan (HSPG) Syndecan-3 are expressed in the dorsal medial hypothalamus together with LepR [28]. Nevertheless, research into the specific involvement of HS in leptin signaling remains limited, its function is not completely understood and requires further investigation.

Recent studies underscore the pivotal role of HSPG in the endocytosis process. HS chains on HSPGs regulate endocytosis by binding to various ligands such as fibroblast growth factor (FGF) 2, DNA-peptide polyplexes, and very-low-density lipoprotein on the cell surface, facilitating their internalization into cells [29–32]. In addition, cell surface HSPGs facilitate the internalization of recombinant human bone morphogenetic protein [33]. HSPG also serves as a receptor for coronaviruses, including SARS-CoV-2, during their entry into host cells [34]. Furthermore, studies have demonstrated that HSPGs regulate the endocytosis of specific morphogens like *Drosophila* Decapentaplegic [35,36]. Glypican, a member of the HSPG family, plays a crucial role in the Decapentaplegic signaling pathway and endocytosis mechanisms independent of dynamin-mediated processes. Thus, HSPGs mediate endocytosis through various pathways, including caveolin-dependent and clathrin-dependent mechanisms and macropinocytosis [37].

This study explores the role of HS in leptin signaling. We demonstrated that cell surface HS modulates leptin signaling in Neuro2A cells expressing full-length LepR. In addition, we observed that cell surface HS regulates LepR expression after leptin exposure. Importantly, we found that cell surface HS inhibits the interaction between LepR and Lrp1. Our findings suggest that cell surface HS restricts the interaction between LepR and Lrp1, influencing LepR pool dynamics by affecting its endocytosis, recycling and thereby impacting leptin signaling.

2. Material and methods

2.1. Materials

Three clones of Neuro2A cells expressing full-length human LepR (Neuro2A-ObRb) were generated through transfection of Halo-tag-conjugated full-length human LepR into Neuro2A cells. All clones were utilized for the experiments presented in Figures 1 and 2, and consistent results were obtained. Subsequently, one representative clone was selected for the remaining experiments. The 293T cells were

obtained from the RIKEN-BRC. Recombinant human leptin was purchased from Peprotech, and heparin was supplied by Seikagaku Corporation. The antibodies employed in this study included: mouse monoclonal (IgM) anti-heparan sulfate F58-10E4 antibody (Seikagaku Corporation); rabbit monoclonal anti-phospho-STAT3 (pSTAT3) antibody (D3A7); mouse monoclonal anti-STAT3 antibody (124H6); rabbit polyclonal anti-phospho-SHP2 (Tyr542); rabbit monoclonal anti-SHP2 (D50F2); rabbit monoclonal anti-phospho-p44/42 MAPK(Erk1/2) (Thr202/Tyr204) (D13.14.4E); rabbit monoclonal anti-syntaxin6 antibody (C34B2); rabbit monoclonal anti-EEA1 antibody (C45B10); rabbit monoclonal anti-clathrin antibody (D3C6); rabbit monoclonal anti-APPL1 antibody (D83H4) (Cell Signaling Technologies); mouse monoclonal anti-Lrp1 antibody (11H4) (BioLegend); three types of antibodies against the LepR: rabbit polyclonal antibodies (Proteintech and Genetex) and a mouse monoclonal antibody (Santa Cruz Biotechnology); HRP-conjugated anti-mouse and anti-rabbit IgG (MP Biomedicals); Alexa 488-conjugated goat anti-mouse IgM antibody, Alexa 594-conjugated goat anti-rabbit IgG antibody, and Alexa 594-conjugated streptavidin (ThermoFisher Scientific). Heparinase, heparitinase I, and heparitinase II from *Flavobacterium heparinum*, as well as an unsaturated heparan sulfate disaccharide kit, were purchased from Seikagaku Corporation.

2.2. Western blotting

Cells were lysed directly in Leammli's sample buffer supplemented with 10 mM dithiothreitol. Protein concentrations were determined using a micro BCA™ protein assay kit (ThermoFisher Scientific). Equal amounts of protein (20–40 μg) were separated by SDS-PAGE on 8% polyacrylamide gels and transferred onto Immobilon-P PVDF membranes (Millipore) using a wet tank transfer apparatus (NIHON EIDO Corp.) with transfer buffer (25 mM Tris, 100 mM glycine, and 20% (v/v) methanol) at 10 V/gel overnight. Following transfer, membranes were blocked with 5% nonfat dry milk in TBST (20 mM Tris-HCl, 150 mM NaCl, 0.1% Tween-20, pH 7.5) for 1 h at room temperature. Primary antibodies were

applied at the recommended dilution ratio provided by the manufacturer in Can Get Signal® solution 1 (TOYOBO) and incubated overnight at 4˚C. After three washes with TBST, membranes were incubated with HRP-conjugated secondary antibodies (diluted 1:2000 in Can Get Signal® solution 2 (TOYOBO)) for 1 h at room temperature. Following three additional washes with TBST, signals were detected using Western Lightning® ECL Pro detection reagent (PerkinElmer) and visualized with a chemiluminescence imaging system, ImageQuant™ LAS4000 mini (Cytiva). Band intensities were quantified using ImageJ BandPeak Quantification [38].

2.3. Immunocytochemistry

Cells were seeded on coverslips and fixed with 4% paraformaldehyde in phosphate-buffered saline (PBS) for 15 min at room temperature. After fixation, cells were washed three times with PBS, permeabilized with 0.2% Triton X-100 in PBS for 3 min, and then blocked with blocking buffer (1% Bovine Serum Albumin (Sigma) in PBS) for 1 h at room temperature to minimize non-specific antibody binding. Subsequently, cells were incubated overnight at 4°C with primary antibodies diluted in blocking buffer (following the manufacturer's recommended dilution ratio). After incubation, cells were washed three times with PBS and then incubated with fluorescently labeled secondary antibodies (diluted 1:1000 in blocking buffer) for 1 h at room temperature. After three washes with PBS, cells were counterstained with 4',6-diamidino-2-phenylindole (DAPI, 1 µg/mL) for 5 min at room temperature. Coverslips were mounted onto glass slides using Fluoromount Aqueous Mounting Medium (Sigma) and allowed to air-dry. Imaging was performed using the FV3000 confocal microscope (EVIDENT) and subsequent analysis was conducted using ImageJ software.

2.4. Flow Cytometry (FACS)

Cells treated with HS-degrading enzymes (HSases) and/or leptin were detached using Accutase (Nacalai Tesque), washed twice with PBS, and fixed with 4% paraformaldehyde in PBS for 15 min at room temperature. To minimize non-specific binding, cells were then incubated with 1% BSA for 1 h at 4°C. Next, cells were exposed to anti-LepR antibodies (Genetex) for 1 h at 4°C, followed by two washes with PBS and subsequent incubation with Alexa 488-conjugated secondary antibodies for 1 h at 4°C. Then, cells underwent three washes with PBS to remove unbound antibodies. The cells were resuspended in PBS and analyzed using a NovoCyte flow cytometer (Agilent). Each sample collected a minimum of 10,000 events for analysis, and flow cytometry data were processed using the software supplied by the manufacturer.

2.5. Immunoprecipitation

Cells were lysed in RIPA lysis buffer (50 mM Tris-HCl, 150 mM NaCl, 1% NP-40, 0.5% sodium deoxycholate, 0.1% sodium dodecyl sulfate, pH 8.0), supplemented with cOmplete™ Protease Inhibitor Cocktail (Merck) at the manufacturer-recommended concentration. Lysates were incubated on ice for 30 min and then clarified by centrifugation at 12,000 × g for 20 min at 4°C. The resulting supernatants were collected for further analysis. Equal amounts of protein (500 µg) from the supernatants were incubated overnight at 4°C with gentle rotation with primary antibodies specific to LepR (anti-LepR (Proteintech) or anti-Ob-R (Santa Cruz Biotechnology). Subsequently, 20 µL of Dynabeads™ protein G (Invitrogen) was added to the mixture, followed by an additional 1 h incubation at room temperature under gentle rotation. The beads were washed three times with TBST to remove non-specifically bound proteins. After the final wash, the beads were resuspended in an SDS sample buffer containing 50 mM dithiothreitol and then boiled. The proteins were separated by SDS-PAGE on an 8% polyacrylamide gel, transferred onto a PVDF membrane, and subjected to Western blotting.

2.6. Interaction analysis between HS and LepR

Cell lysates were prepared as described previously. A mixture of heparin solution (100 µL of 10 mg/mL in PBS) and 1 mg of Sulfo-SBED Biotin Label Transfer Reagent (ThermoFisher Scientific) was incubated at room temperature 1 h to facilitate labeling. Excess Sulfo-SBED was removed by ultrafiltration using a device with a molecular weight cut-off of 10,000. The reaction mixture was washed twice with 300 µL of PBS during ultrafiltration. The resulting heparin (100 µg of Hep-SBED) was combined with 1 mg of cell lysate (1 mg/mL). Proteins interacting with Hep-SBED were crosslinked using a UV transilluminator set at 365 nm wavelength for 5 min. The lysates were then incubated overnight at 4°C with 20 µL of anti-FLAG M2 affinity agarose gel. After incubation, the agarose beads were washed three times with PBS and stained with Alexa-594 conjugated streptavidin in PBS (1/1000 dilution). The beads were resuspended in 300 µL of PBS and transferred to a 48-well plate. Images were captured using the BZ-X800 fluorescence microscope (KEYENCE) and analyzed using the software supplied by the manufacturer.

3. Results

3.1. Decreased leptin signaling in HS-depleted cells

HS plays an important role in regulating various signaling pathways by interacting with ligands and receptors as a glycosaminoglycan chain of HSPG on the cell surface. In this study, we investigated the influence of cell surface HS on leptin signaling using a mouse neuroblastoma cell line (Neuro2A) as a model system. These cells naturally express HSPGs with HS chains, but lack LepR, making them unresponsive to leptin. To explore leptin signal transduction, we introduced the full-length LepR into Neuro2A cells (designated as Neuro2A-ObRb) and assessed their response to leptin stimulation. We focused on the role of HS chains on HSPGs in regulating leptin signaling pathways by examining

changes in downstream signaling molecules. Western blotting analysis revealed activation of downstream molecules such as STAT3, SHP2, and ERK1/2 upon leptin treatment, indicating that Neuro2A cells possess the machinery for leptin signaling (Fig. 1C). To investigate the role of cell surface HS in regulating leptin signaling, HS was removed enzymatically from the cell surface using a mixture of enzymes, including Heparinase (1 mU/mL), heparitinase I (1 mU/mL), and heparitinase II (0.5 mU/mL) from *Flavobacterium heparinum*, as shown in Figure 1B. Immunostaining with the 10E4 antibody showed robust fluorescence in untreated cells, confirming the presence of HS chains on HSPGs. However, fluorescence was notably reduced in cells treated with HSases, indicating a substantial decrease in cell surface HS (Fig. 1A). FACS analysis further quantified this reduction, showing a significant decrease in 10E4 staining intensity in treated cells compared to untreated ones (Supplementary Fig. 2). Under these conditions, Western blotting analysis revealed decreased levels of phosphorylated STAT3, SHP2, and pERK in HSases-treated cells compared to untreated cells (Fig. 1C, D). This reduction in phosphorylated proteins suggests impaired leptin signal transduction in the absence of cell surface HS. To further investigate, we generated a pool of cells with *Ext1* knocked out via genome editing (Supplementary Fig. 3). Immunostaining with the 10E4 antibody showed reduced fluorescence in *Ext1* knocked out cells, indicating a substantial decrease in cell surface HS (Supplementary Fig. 3A). Disaccharide analysis showed that HS was reduced from 346.45 to 159.53 pmol/mg protein in these cells. Due to the limitations in expanding the mixture of *Ext1* knockdown cells, an insufficient number of cells was available for triplicate experiments, and thus the experiment was conducted only once. We analyzed the phosphorylation of STAT3, ERK1/2, and SHP-2. Interestingly, in Ext1 knockout cells, the basal phosphorylation level of STAT3 was 7.2 times higher than normal, even without leptin treatment, and it increased further with leptin treatment. However, the fold increase from the basal state was significantly lower in *Ext1* knockout cells (90.2, 70.0, 55.4, 30.1 for parental cells; 9.1, 5.7, 5.9, 4.3 for Ext1 knockout cells, $p < 0.05$, Welch's t-test). ERK1/2 phosphorylation was comparable to levels observed with leptin

treatment, even in the absence of leptin. A significant decrease in phosphorylated SHP-2 was observed in the knockout cells compared with parental cells. The findings further confirm that the absence of HS impairs leptin signaling.

To explore the impact of cell surface chondroitin sulfate (CS) on leptin signaling, we first quantified the levels of CS using disaccharide analysis (Supplementary Fig. 1). Disaccharide analysis showed minimal accumulation of chondroitin sulfate (CS) (~0.5 pmol/μg protein) under our experimental conditions, compared to approximately 20 pmol/μg protein observed in mesenchymal stem cells (data not shown). Cells were treated with chondroitinase ABC (CHase ABC) to further reduce CS levels, achieving approximately a 50% reduction. Despite this reduction, the induction of phosphorylated STAT3 (pSTAT3) upon leptin stimulation showed no significant difference between CHase ABC-treated and untreated cells. These findings suggest that under our experimental conditions, where cell surface CS accumulation is minimal, CS does not play a critical role in modulating the STAT3 activation pathway in response to leptin.

3.2. Effect of HS chains on LepR cell surface expression

To evaluate the impact of HS chains on HSPGs on LepR expression, we performed FACS analysis. In cells untreated with HSases, LepR expression on the cell surface remained unchanged at both 0 and 90 min following leptin addition (Fig. 2A). Conversely, cells treated with HSases exhibited a significant reduction in fluorescence at 90 min post-leptin addition, indicating a decrease in cell surface LepR expression (Fig. 2A). Moreover, immunostaining of intracellular LepR showed a gradual decline in LepR levels over time in cells without HSases treatment, whereas no significant change was observed from 0 to 90 min in cells treated with HSases (Fig. 2B). These findings suggest that cell surface HS is involved in regulating both cell surface and intracellular LepR expression. Next, we investigated whether the addition of leptin affected HS localization. In cells untreated with HSases, HS was transiently observed around the

nucleus 15 min after leptin treatment and diminished after 90 min of treatment (Fig. 3A, upper panels). Conversely, cells pre-treated with HSases showed no detectable changes in nuclear peripheral HS (Fig. 3A, lower panels). Intracellular HS partially co-localized with the Golgi marker Syntaxin6 and the endosomal markers EEA1 and Clathrin, indicating the presence of HS in the Golgi apparatus and endosomes (Fig. 3B, arrowheads). HS and LepR displayed slight co-localization both intracellularly (Fig. 3C) and extracellularly (Fig. 3D). These findings suggest that leptin induces changes in intracellular HS localization without a significant interaction between HS and LepR.

3.3. Interaction between LepR and Heparin

We identified several potential heparin-binding motifs in mouse LepR, including RSKR at positions 306-310, KATRPRGK at positions 394-402, RCRR at positions 609-613, and RMKK at positions 863-867. However, these interactions were not detectable using standard enzyme-linked immunosorbent assays (ELISA), likely because they were not sufficiently robust to withstand the washing steps and other manipulations typical of ELISA. To address this limitation, we employed a combination of visible immunoprecipitation and interaction analysis using a photoreactive crosslinker, which allowed us to analyze conditions more closely resembling those in living cells [39]. The extracellular domain of LepR or HS6ST3, tagged with FLAG, was expressed in 293T cells (Fig. 4A). To test the potential interaction of heparin with these proteins, cell lysates were incubated with Hep-SBED. For specificity testing, an equal amount of free heparin was added as a competitor. After photo-crosslinking the proteins that interact with heparin, the FLAG fusion proteins were bound to M2 agarose beads. The beads were then washed, stained, and observed for fluorescence. We used HS6ST3 as a positive control because HS6ST was purified based on its ability to bind heparin [40]. The beads coupled with FLAG-HS6ST3 and FLAG-LepRΔC showed a significant increase in fluorescence intensity, indicating that Hep-SBED specifically bound to and crosslinked HS6ST3 and LepRΔC (Fig. 4B, C). When cold heparin was added as a

competitor during the interaction, there was no increase in fluorescence intensity. These results suggest that LepR interacts with heparin.

3.4. HS-dependent interaction between LepR and Lrp1

Given the role of Lrp proteins in regulating LepR endocytosis, we next investigated whether the interaction between LepR and Lrp1 is dependent on HS. In Neuro2A-ObRb cells, both LepR and Lrp1 were expressed at similar levels regardless of HSases treatment or leptin addition (Fig. 5A, C). Immunoprecipitation with two different antibodies targeting LepR, followed by immunoblotting for LepR and Lrp1, showed that LepR levels in the immunoprecipitates were comparable across all treatments (Fig. 5B, E). Interestingly, when cells were treated with leptin after removal of HS from the cell surface, a greater amount of Lrp1 was detected in the immunoprecipitates than in cells untreated with HSases (Fig. 5D, E). These results suggest that the interaction between LepR and Lrp1 increases when the cell surface HS is removed, indicating that HS serves as a negative regulator of this interaction.

To further investigate the potential functional relationship between Lrp1 and cell surface HS in leptin signaling, we conducted *Lrp1* siRNA knockdown experiments (Supplemental Figures 4 and 5). Following siRNA treatment, we observed a significant reduction in both *Lrp1* mRNA (Supplemental Figures 4A and 5A) and protein levels. Upon leptin treatment, the parental cells exhibited an increase in cell surface LepR expression 30 minutes post-treatment. In contrast, this increase was not observed in *Lrp1* knockdown cells (Supplemental Figures 4B). Additionally, the induction of phosphorylated STAT3, a downstream marker of leptin signaling, was decreased in *Lrp1* knockdown cells compared to parental cells (Supplemental Figures 5B). The lack of increased cell surface LepR expression and reduced phosphorylated STAT3 induction in *Lrp1* knockdown cells suggest that both Lrp1 and cell surface HS share a similar role in regulating LepR-mediated leptin signaling.

4. Discussion

Leptin signaling is crucial for maintaining energy homeostasis and regulating body weight. However, the potential role of HS in leptin signaling has not been explored. In the present study, we show that cell surface HS is involved in leptin signaling by modulating the number of cell surface leptin receptors. This study is significant given the similar expression patterns of LepR, HS-modifying enzymes such as HS6ST2, and one of the HSPGs, Syndecan-3, in the hypothalamus [28]. In addition, we observed weaker STAT3 activation in *Hs6st2* knockout mice compared to wild-type mice after leptin administration (manuscript in preparation), indicating a vital role for HS in the leptin signaling pathway [27,41]. Therefore, the results of this study could provide new insights into the mechanisms underlying metabolic abnormalities and the treatment of obesity.

We demonstrated that cell surface HS regulates leptin signaling in cell-based experiments. Leptin activates key signaling pathways, such as JAK-STAT, MAPK, and PI3K-Akt signaling pathways, which are essential for maintaining the energy balance. Our data show that removing cell surface HS attenuates the JAK-STAT pathway (Fig. 1) and reduces the amount of cell surface LepR (Fig. 2). These findings suggest that cell surface HS enhances leptin signaling by retaining LepR on the cell surface. In comparison, *Ext1* knockout cells showed decreased phosphorylation of SHP-2, although STAT3 and ERK phosphorylation were elevated even in the absence of leptin, indicating altered cellular states that complicate interpretation (Supplementary Fig. 3). Nonetheless, the lower induction ratio of STAT3, along with the SHP-2 results, suggests that leptin signaling is weakened as is observed in enzymatic digestion.

There are known examples of HS interacting with ligands and receptors to stabilize complex formation. For instance, HS chains on HSPGs have been shown to stabilize FGF receptors by interacting with both FGF receptor 1 and FGF2, forming a ternary complex that enhances receptor dimerization and facilitates efficient signal transduction [42] [43]. Similarly, in the Wnt signaling pathway, HSPG helps retain Frizzled receptors on the cell surface, promoting Wnt ligand binding and downstream signaling

[44]. However, since there appears to be no interaction between leptin and HS [45], and the interaction with LepR is likely very weak (Fig. 4), a different mechanism is likely involved. Unlike in the cases of FGF and Wnt, where interaction with HS chains on HSPGs stabilize the complex and enhances signal transduction, the role of HS in leptin signaling seems to follow a distinct pathway.

Our findings indicated that removing HS from the cell surface increased the amount of Lrp1 in the LepR immunoprecipitates (Fig. 5), suggesting that HS inhibits the binding between LepR and Lrp1. Lrp1 is known to regulate the endocytosis and recycling of various large molecules, including integrin [46]. It interacts with the glycan chains of HSPGs, and HS chains play a role in the regulation of Lrp1-mediated endocytosis [47,48]. This interaction likely plays a crucial role in modulating the availability and function of Lrp1 on the cell surface. Lrp2, a family member of Lrp1, has been implicated in controlling LepR endocytosis and leptin-induced hypothalamic Stat3 activation [14]. Considering the established role of Lrp1 in endocytosis and its potential interaction with HSPGs, HS chains on HSPG may function as regulatory molecules, modulating the binding between Lrp1 and LepR. This interaction may affect the internalization of LepR and its subsequent signaling pathways. Considering that Lrp1 knockdown does not lead to an increase in cell surface LepR 30 minutes after leptin addition (Supplementary Figure 4), we propose a hypothesis (Graphical Abstract) that Lrp1, in coordination with HSPG, may play a role in presenting LepR on the cell surface. In the absence of HS chains on HSPGs, the internalized Lrp1-LepR complex may be unable to transition to more acidic compartments and dissociate, preventing its recycling back to the cell surface. As a result, the Lrp1-LepR complex is likely to accumulate within the cell. This could result in a decrease in cell surface leptin receptors, potentially impacting leptin signaling. Such a mechanism suggests that HS chains on HSPG might play a critical role in the trafficking and recycling of LepR, influencing the receptor's availability and responsiveness to leptin.

Our findings further revealed that leptin treatment triggers a transient increase in perinuclear HS after 15 minutes, which diminishes by 90 minutes. Conversely, cells treated with HSases show no significant changes in perinuclear HS. The partial co-localization with intracellular markers (Fig. 3) suggests that HS is present in the Golgi apparatus and endosomes, implying a potential role in intracellular trafficking. There are other instances where HSPGs are internalized upon ligand addition [37]. For example, the anti-DNA autoantibody 3D8 scFv binds to cell surface HSPGs and internalizes into cells, co-localizing with HS and caveolin-1 [49]. Mandarini et al. demonstrated that HSPGs undergo endocytosis with NT4 (a peptide mimicking heparin-binding ligand) and translocated to endosomes [50]. Considering that intracellular LepR levels gradually decrease in control cells but remain stable in HSases-treated cells, intracellular HS may influence the recycling of LepR to the plasma membrane or its intracellular degradation processes. We hypothesize that HS chains, internalized along with LepR, is crucial for the sorting of internalized LepR back to the cell surface in conjunction with Lrp1. This mechanism could ensure the efficient return of LepR to the cell surface, maintaining receptor availability and thus regulating leptin signaling. However, due to the difficulty in directly proving the interaction between HS and Lrp1, further research is needed to fully elucidate how this interaction impacts the dynamics and signaling of LepR. Future studies should focus on identifying the precise molecular mechanisms by which HS chains on HSPGs modulate Lrp1 and LepR interactions and their implications for leptin signaling pathways. Additionally, our data do not yet elucidate the precise role of intracellular HS in leptin signaling, and further research is needed to confirm these mechanistic insights.

Our study provides strong evidence for the involvement of cell surface HS in leptin signaling; however, several limitations remain. First, we did not fully analyze the direct interaction between HS and LepR. While our modified visual immunoprecipitation assay using Hep-SBED showed an interaction between heparin and LepR, a more detailed investigation between HS and LepR using techniques like surface plasmon resonance or isothermal titration calorimetry is warranted. In addition, since LepR forms

multimeric complexes at the cell surface, binding assays with HS should incorporate the LepR complex. Second, the significance of HS modification and core proteins remains unclear. Identifying HS-modifying enzymes and core proteins involved in leptin signaling is crucial for a more comprehensive understanding of HS's role in this process.

5. Conclusion

In conclusion, our findings suggest that cell surface HS plays a critical role in regulating LepR signaling. Cell surface HS affects the amount of LepR expressed on the cell surface by influencing its endocytosis or recycling through inhibition of its interaction with Lrp1. Our results underscore the importance of HS chains on HSPGs in leptin function and contribute to a deeper understanding of leptin signaling mechanisms. Future studies will further enrich our understanding of leptin signaling and may unveil new therapeutic targets for metabolic disorders and obesity.

Funding

This work was supported by JSPS KAKENHI Grant Numbers 21K08588 and 24K11708 to NN and 21H02720 to HW.

CRedTt authorship contribution statement

Naoko Nagai: Conceptualization, Writing – original draft, Investigation, Ran experiments, and Data Analysis.

Tatsumasa Shioiri: Ran experiments and Validation

Sonoko Hatano: Investigation and Visualization

Nobuo Sugiura: Methodology, Investigation and Resources.

Hideto Watanabe: Writing – review, Funding acquisition and Supervision.

Declaration of competing interests

Naoko Nagai and Hideto Watanabe acknowledge financial support from the Japan Society for the Promotion of Science. We confirm that we have no known competing financial interests or personal relationships that could have influenced the work reported in this paper.

Declaration of generative AI and AI-assisted technologies in the writing process

During the preparation of this study, the authors used GPT-4o and DeepL to enhance the readability and language of the manuscript. Following this, we reviewed and edited the content as needed, and we take full responsibility for the content of the published article.

Acknowledgement

We thank Makoto Naruse (Aichi Medical University, Institute of Comprehensive Medical Research, Division of Advanced Research Promotion) for his assistance in cell cloning. We appreciate the discussions with Takashi Kobayashi, and Jun Tsuchimoto, as well as the support from Keiko Ota with administrative procedures. In addition, we acknowledge Koji Kimata and Hiroko Habuchi for their longstanding collaboration and valuable insights. We would like to thank Enago (www.enago.jp) for the English language review.

Data availability statement

All data in our study are available upon reasonable request.

References

[1] Y. Zhang, R. Proenca, M. Maffei, M. Barone, L. Leopold, J.M. Friedman, Positional cloning of the mouse obese gene and its human homologue, Nature 372 (1994) 425–432. https://doi.org/10.1038/372425a0.

[2] R.S. Ahima, J.S. Flier, Leptin, Annu. Rev. Physiol. 62 (2000) 413–437. https://doi.org/10.1146/annurev.physiol.62.1.413.

[3] M.G. Myers, M.A. Cowley, H. Münzberg, Mechanisms of Leptin Action and Leptin Resistance, Annu. Rev. Physiol. 70 (2008) 537–556. https://doi.org/10.1146/annurev.physiol.70.113006.100707.

[4] H.-K. Park, R.S. Ahima, Leptin signaling, F1000Prime Rep. 6 (2014). https://doi.org/10.12703/P6-73.

[5] H.-K. Park, R.S. Ahima, Physiology of leptin: energy homeostasis, neuroendocrine function and metabolism, Metabolism 64 (2015) 24–34. https://doi.org/10.1016/j.metabol.2014.08.004.

[6] A. Sahu, Leptin signaling in the hypothalamus: emphasis on energy homeostasis and leptin resistance, Front. Neuroendocrinol. 24 (2003) 225–253. https://doi.org/10.1016/j.yfrne.2003.10.001.

[7] B.F. Belgardt, J.C. Brüning, CNS leptin and insulin action in the control of energy homeostasis, Ann. N. Y. Acad. Sci. 1212 (2010) 97–113. https://doi.org/10.1111/j.1749-6632.2010.05799.x.

[8] A.A. Barrios-Correa, J.A. Estrada, I. Contreras, Leptin Signaling in the Control of Metabolism and Appetite: Lessons from Animal Models, J. Mol. Neurosci. 66 (2018) 390–402. https://doi.org/10.1007/s12031-018-1185-0.

[9] J.M. Friedman, Leptin and the endocrine control of energy balance, Nat. Metab. 1 (2019) 754–764. https://doi.org/10.1038/s42255-019-0095-y.

[10] C. Vaisse, J.L. Halaas, C.M. Horvath, J.E. Darnell, M. Stoffel, J.M. Friedman, Leptin activation of Stat3 in the hypothalamus of wild–type and ob/ob mice but not db/db mice, Nat. Genet. 14 (1996) 95–97. https://doi.org/10.1038/ng0996-95.

[11] C. Bjørbæk, R.M. Buchholz, S.M. Davis, S.H. Bates, D.D. Pierroz, H. Gu, B.G. Neel, M.G. Myers, J.S. Flier, Divergent Roles of SHP-2 in ERK Activation by Leptin Receptors, J. Biol. Chem. 276 (2001) 4747–4755. https://doi.org/10.1074/jbc.M007439200.

[12] G. Frühbeck, Intracellular signalling pathways activated by leptin, Biochem. J. 393 (2006) 7–20. https://doi.org/10.1042/BJ20051578.

[13] S. Belouzard, D. Delcroix, Y. Rouillé, Low Levels of Expression of Leptin Receptor at the Cell Surface Result from Constitutive Endocytosis and Intracellular Retention in the Biosynthetic Pathway, J. Biol. Chem. 279 (2004) 28499–28508. https://doi.org/10.1074/jbc.M400508200.

[14] K. Byun, S.Y. Gil, C. Namkoong, B. Youn, H. Huang, M. Shin, G.M. Kang, H. Kim, B. Lee, Y. Kim, M. Kim, Clusterin/ApoJ enhances central leptin signaling through Lrp2-mediated endocytosis, EMBO Rep. 15 (2014) 801–808. https://doi.org/10.15252/embr.201338317.

[15] S.Y. Gil, B.-S. Youn, K. Byun, H. Huang, C. Namkoong, P.-G. Jang, J.-Y. Lee, Y.-H. Jo, G.M. Kang, H.-K. Kim, M.-S. Shin, C.U. Pietrzik, B. Lee, Y.-B. Kim, M.-S. Kim, Clusterin and LRP2 are critical components of the hypothalamic feeding regulatory pathway, Nat. Commun. 4 (2013) 1862. https://doi.org/10.1038/ncomms2896.

[16] O. Kwon, K.W. Kim, M.-S. Kim, Leptin signalling pathways in hypothalamic neurons, Cell. Mol. Life Sci. 73 (2016) 1457–1477. https://doi.org/10.1007/s00018-016-2133-1.

[17] M. Bernfield, M. Götte, P.W. Park, O. Reizes, M.L. Fitzgerald, J. Lincecum, M. Zako, Functions of Cell Surface Heparan Sulfate Proteoglycans, Annu. Rev. Biochem. 68 (1999) 729–777. https://doi.org/10.1146/annurev.biochem.68.1.729.

[18] B. Casu, U. Lindahl, Structure and biological interactions of heparin and heparan sulfate, in: Adv. Carbohydr. Chem. Biochem., Elsevier, 2001: pp. 159–206. https://doi.org/10.1016/S0065-2318(01)57017-1.

[19] U. Lindahl, M. Kusche-Gullberg, L. Kjellén, Regulated Diversity of Heparan Sulfate, J. Biol. Chem. 273 (1998) 24979–24982. https://doi.org/10.1074/jbc.273.39.24979.

[20] J.D. Esko, U. Lindahl, Molecular diversity of heparan sulfate, J. Clin. Invest. 108 (2001) 169–173. https://doi.org/10.1172/JCI200113530.

[21] D. Xu, J.D. Esko, Demystifying Heparan Sulfate–Protein Interactions, Annu. Rev. Biochem. 83 (2014) 129–157. https://doi.org/10.1146/annurev-biochem-060713-035314.

[22] J. Kreuger, D. Spillmann, J. Li, U. Lindahl, Interactions between heparan sulfate and proteins: the concept of specificity, J. Cell Biol. 174 (2006) 323–327. https://doi.org/10.1083/jcb.200604035.

[23] M. Inatani, F. Irie, A.S. Plump, M. Tessier-Lavigne, Y. Yamaguchi, Mammalian Brain Morphogenesis and Midline Axon Guidance Require Heparan Sulfate, Science 302 (2003) 1044–1046. https://doi.org/10.1126/science.1090497.

[24] S.E. Lauri, S. Kaukinen, T. Kinnunen, A. Ylinen, S. Imai, K. Kaila, T. Taira, H. Rauvala, Reg1ulatory Role and Molecular Interactions of a Cell-Surface Heparan Sulfate Proteoglycan (*N* -syndecan) in Hippocampal Long-Term Potentiation, J. Neurosci. 19 (1999) 1226–1235. https://doi.org/10.1523/JNEUROSCI.19-04-01226.1999.

[25] M. Kaksonen, I. Pavlov, V. Võikar, S.E. Lauri, A. Hienola, R. Riekki, M. Lakso, T. Taira, H. Rauvala, Syndecan-3-Deficient Mice Exhibit Enhanced LTP and Impaired Hippocampus-Dependent Memory, Mol. Cell. Neurosci. 21 (2002) 158–172. https://doi.org/10.1006/mcne.2002.1167.

[26] Y. Yamaguchi, M. Inatani, Y. Matsumoto, J. Ogawa, F. Irie, Roles of Heparan Sulfate in Mammalian Brain Development, in: Prog. Mol. Biol. Transl. Sci., Elsevier, 2010: pp. 133–152. https://doi.org/10.1016/S1877-1173(10)93007-X.

[27] S. Moon, H.H. Lee, S. Archer-Hartmann, N. Nagai, Z. Mubasher, M. Parappurath, L. Ahmed, R.L. Ramos, K. Kimata, P. Azadi, W. Cai, J.Y. Zhao, Knockout of the intellectual disability-linked gene *Hs6st2* in mice decreases heparan sulfate 6-O-sulfation, impairs dendritic spines of hippocampal neurons, and affects memory, Glycobiology 34 (2024) cwad095. https://doi.org/10.1093/glycob/cwad095.

[28] E.S. Lein, M.J. Hawrylycz, N. Ao, M. Ayres, A. Bensinger, A. Bernard, A.F. Boe, M.S. Boguski, K.S. Brockway, E.J. Byrnes, L. Chen, L. Chen, T.-M. Chen, M. Chi Chin, J. Chong, B.E. Crook, A. Czaplinska, C.N. Dang, S. Datta, N.R. Dee, A.L. Desaki, T. Desta, E. Diep, T.A. Dolbeare, M.J. Donelan, H.-W. Dong, J.G. Dougherty, B.J. Duncan, A.J. Ebbert, G. Eichele, L.K. Estin, C. Faber, B.A. Facer, R. Fields, S.R. Fischer, T.P. Fliss, C. Frensley, S.N. Gates, K.J. Glattfelder, K.R. Halverson, M.R. Hart, J.G. Hohmann, M.P. Howell, D.P. Jeung, R.A. Johnson, P.T. Karr, R. Kawal, J.M. Kidney, R.H. Knapik, C.L. Kuan, J.H. Lake, A.R. Laramee, K.D. Larsen, C. Lau, T.A. Lemon, A.J. Liang, Y. Liu, L.T. Luong, J. Michaels, J.J. Morgan, R.J. Morgan, M.T. Mortrud, N.F. Mosqueda, L.L. Ng, R. Ng, G.J. Orta, C.C. Overly, T.H. Pak, S.E. Parry, S.D. Pathak, O.C. Pearson, R.B. Puchalski, Z.L. Riley, H.R. Rockett, S.A. Rowland, J.J. Royall, M.J. Ruiz, N.R. Sarno, K. Schaffnit, N.V. Shapovalova, T. Sivisay, C.R. Slaughterbeck, S.C. Smith, K.A. Smith, B.I. Smith, A.J. Sodt, N.N. Stewart, K.-R. Stumpf, S.M. Sunkin, M. Sutram, A. Tam, C.D. Teemer, C. Thaller, C.L. Thompson, L.R. Varnam, A. Visel, R.M. Whitlock, P.E. Wohnoutka, C.K. Wolkey, V.Y. Wong, M. Wood, M.B. Yaylaoglu, R.C. Young, B.L. Youngstrom, X. Feng Yuan, B. Zhang, T.A. Zwingman, A.R. Jones, Genome-wide atlas of gene expression in the adult mouse brain, Nature 445 (2007) 168–176. https://doi.org/10.1038/nature05453.

[29] E. Tkachenko, E. Lutgens, R.-V. Stan, M. Simons, Fibroblast growth factor 2 endocytosis in endothelial cells proceed via syndecan-4-dependent activation of Rac1 and a Cdc42-dependent macropinocytic pathway, J. Cell Sci. 117 (2004) 3189–3199. https://doi.org/10.1242/jcs.01190.

[30] L.C. Wilsie, A.M. Gonzales, R.A. Orlando, Syndecan-1 mediates internalization of apoE-VLDL through a low density lipoprotein receptor-related protein (LRP)-independent, non-clathrin-mediated pathway, Lipids Health Dis. 5 (2006) 23. https://doi.org/10.1186/1476-511X-5-23.

[31] S. Paris, A. Burlacu, Y. Durocher, Opposing Roles of Syndecan-1 and Syndecan-2 in Polyethyleneimine-mediated Gene Delivery, J. Biol. Chem. 283 (2008) 7697–7704. https://doi.org/10.1074/jbc.M705424200.

[32] A. Wittrup, S.-H. Zhang, K.J. Svensson, P. Kucharzewska, M.C. Johansson, M. Mörgelin, M. Belting, Magnetic nanoparticle-based isolation of endocytic vesicles reveals a role of the heat shock protein GRP75 in macromolecular delivery, Proc. Natl. Acad. Sci. 107 (2010) 13342–13347. https://doi.org/10.1073/pnas.1002622107.

[33] M.G. Kim, C.L. Kim, Y.S. Kim, J.W. Jang, G.M. Lee, Selective endocytosis of recombinant human BMPs through cell surface heparan sulfate proteoglycans in CHO cells: BMP-2 and BMP-7, Sci. Rep. 11 (2021) 3378. https://doi.org/10.1038/s41598-021-82955-1.

[34] M. Bermejo-Jambrina, J. Eder, T.M. Kaptein, J.L. Van Hamme, L.C. Helgers, K.E. Vlaming, P.J.M. Brouwer, A.C. Van Nuenen, M. Spaargaren, G.J. De Bree, B.M. Nijmeijer, N.A. Kootstra, M.J. Van Gils, R.W. Sanders, T.B.H. Geijtenbeek, Infection and transmission of SARS-CoV-2 depend on heparan sulfate proteoglycans, EMBO J. 40 (2021) e106765. https://doi.org/10.15252/embj.2020106765.

[35] T.Y. Belenkaya, C. Han, D. Yan, R.J. Opoka, M. Khodoun, H. Liu, X. Lin, Drosophila Dpp Morphogen Movement Is Independent of Dynamin-Mediated Endocytosis but Regulated by the Glypican Members of Heparan Sulfate Proteoglycans, Cell 119 (2004) 231–244. https://doi.org/10.1016/j.cell.2004.09.031.

[36] N. Simon, A. Safyan, G. Pyrowolakis, S. Matsuda, Dally is not essential for Dpp spreading or internalization but for Dpp stability by antagonizing Tkv-mediated Dpp internalization, eLife 12 (2024) RP86663. https://doi.org/10.7554/eLife.86663.3.

[37] H.C. Christianson, M. Belting, Heparan sulfate proteoglycan as a cell-surface endocytosis receptor, Matrix Biol. 35 (2014) 51–55. https://doi.org/10.1016/j.matbio.2013.10.004.

[38] K. Ohgane, H. Yoshioka, Quantification of Gel Bands by an Image J Macro, Band/Peak Quantification Tool v1, (2019). https://doi.org/10.17504/protocols.io.7vghn3w.

[39] Y. Katoh, S. Nozaki, D. Hartanto, R. Miyano, K. Nakayama, Architectures of multisubunit complexes revealed by a visible immunoprecipitation assay using fluorescent fusion proteins, J. Cell Sci. 128 (2015) 2351–2362. https://doi.org/10.1242/jcs.168740.

[40] H. Habuchi, O. Habuchi, K. Kimata, Purification and Characterization of Heparan Sulfate 6-Sulfotransferase from the Culture Medium of Chinese Hamster Ovary Cells, J. Biol. Chem. 270 (1995) 4172–4179. https://doi.org/10.1074/jbc.270.8.4172.

[41] N. Nagai, H. Habuchi, N. Sugaya, M. Nakamura, T. Imamura, H. Watanabe, K. Kimata, Involvement of heparan sulfate 6-O-sulfation in the regulation of energy metabolism and the alteration of thyroid hormone levels in male mice, Glycobiology 23 (2013) 980–992. https://doi.org/10.1093/glycob/cwt037.

[42] S. Xue, F. Zhou, T. Zhao, H. Zhao, X. Wang, L. Chen, J. Li, S.-Z. Luo, Phase separation on cell surface facilitates bFGF signal transduction with heparan sulphate, Nat. Commun. 13 (2022) 1112. https://doi.org/10.1038/s41467-022-28765-z.

[43] L. Pellegrini, D.F. Burke, F. Von Delft, B. Mulloy, T.L. Blundell, Crystal structure of fibroblast growth factor receptor ectodomain bound to ligand and heparin, Nature 407 (2000) 1029–1034. https://doi.org/10.1038/35039551.

[44] N. Li, L. Wei, X. Liu, H. Bai, Y. Ye, D. Li, N. Li, U. Baxa, Q. Wang, L. Lv, Y. Chen, M. Feng, B. Lee, W. Gao, M. Ho, A Frizzled-Like Cysteine-Rich Domain in Glypican-3 Mediates Wnt

Binding and Regulates Hepatocellular Carcinoma Tumor Growth in Mice, Hepatology 70 (2019) 1231–1245. https://doi.org/10.1002/hep.30646.

[45] O. Reizes, J. Lincecum, Z. Wang, O. Goldberger, L. Huang, M. Kaksonen, R. Ahima, M.T. Hinkes, G.S. Barsh, H. Rauvala, M. Bernfield, Transgenic expression of syndecan-1 uncovers a physiological control of feeding behavior by syndecan-3, Cell 106 (2001) 105–116.

[46] L. Theret, A. Jeanne, B. Langlois, C. Hachet, M. David, M. Khrestchatisky, J. Devy, E. Hervé, S. Almagro, S. Dedieu, Identification of LRP-1 as an endocytosis and recycling receptor for β1-integrin in thyroid cancer cells, Oncotarget 8 (2017) 78614–78632. https://doi.org/10.18632/oncotarget.20201.

[47] M.I. Capurro, W. Shi, J. Filmus, LRP1 mediates the Shh-induced endocytosis of the GPC3-Shh complex, J. Cell Sci. (2012) jcs.098889. https://doi.org/10.1242/jcs.098889.

[48] T. Kanekiyo, J. Zhang, Q. Liu, C.-C. Liu, L. Zhang, G. Bu, Heparan Sulphate Proteoglycan and the Low-Density Lipoprotein Receptor-Related Protein 1 Constitute Major Pathways for Neuronal Amyloid-β Uptake, J. Neurosci. 31 (2011) 1644–1651. https://doi.org/10.1523/JNEUROSCI.5491-10.2011.

[49] H. Park, M. Kim, H.-J. Kim, Y. Lee, Y. Seo, C.D. Pham, J. Lee, S.J. Byun, M.-H. Kwon, Heparan sulfate proteoglycans (HSPGs) and chondroitin sulfate proteoglycans (CSPGs) function as endocytic receptors for an internalizing anti-nucleic acid antibody, Sci. Rep. 7 (2017) 14373. https://doi.org/10.1038/s41598-017-14793-z.

[50] E. Mandarini, E. Tollapi, M. Zanchi, L. Depau, A. Pini, J. Brunetti, L. Bracci, C. Falciani, Endocytosis and Trafficking of Heparan Sulfate Proteoglycans in Triple-Negative Breast Cancer Cells Unraveled with a Polycationic Peptide, Int. J. Mol. Sci. 21 (2020) 8282. https://doi.org/10.3390/ijms21218282.

Figure legend

Figure 1. Impact of HS depletion on leptin signaling in N2A-ObRb cells. A: HSase-treated (+) and untreated (–) N2A-ObRb cells were stained with 10E4 antibody to visualize HS (green). Panels show phase-contrast (left), DAPI staining (middle), and 10E4 staining (right). Scale bar, 50 μm. HS was substantially reduced in HSase-treated cells. B: Time course of treatment with HS-degrading enzymes (HSase) and leptin. HSase was added 30 min before leptin treatment. During the 270-min leptin treatment, HSase was added again at 135 min. Open triangle indicates HSase treatment; closed triangle indicates leptin treatment. C: Activation status of STAT3, SHP2, and ERK1/2 in response to leptin stimulation in both untreated (–HSase) and HSase-treated (+HSase) cells. Cells were either untreated or treated with HSase before leptin stimulation over, as shown in B. Immunoblotting was performed to detect pSTAT3, total STAT3 (STAT3), phospho-SHP2 (pSHP2), total SHP2 (SHP2), phospho-ERK1/2 (pERK1/2), and total ERK1/2 (ERK1/2). Equal amounts of protein extract (23 μg) were used. Molecular weight markers are shown on the right side of the panels. D: Time course of phosphoprotein/total protein is presented as a line graph, normalized to a value of 1 for samples without HSase treatment at t = 0. Data for STAT3 represent the averaged results of three independent experiments with error bars, while data for SHP2 and ERK represent results from two independent experiments, with each measurement indicated by circles (–HSase) and crosses (+HSase). Blue and red lines indicate the results for –HSase and +HSase, respectively. Bars represent the mean ± S.E.M. Statistical significance was determined using Student's t-test between –HSase and +HSase. * $p < 0.05$; ** $p < 0.01$.

Figure 2. Cell surface and intracellular expression of LepR in cells treated with and without HSase. A: Flow cytometry analysis of cell surface LepR expression in cells treated with and without HSase. Cells were either untreated (–HSase) or treated with HSase (+HSase), stimulated with leptin and collected at 0 and 90 min post-stimulation. They were then stained with an anti-LepR antibody to assess cell surface

expression. Fluorescence intensity was measured by flow cytometry and compared. The histogram overlays depicts the changes in fluorescence intensity, indicating LepR expression levels on the cell surface at different time points in both –HSase and +HSase cells. Blue line: Negative control. Red line: 0 min after leptin stimulation. Green line: 90 min after leptin stimulation. B: Immunostaining of intracellular LepR in –HSase and +HSase cells. Cells were either untreated or treated with HSase, then stimulated with leptin. At 0, 30, and 90 min post-stimulation, cells were fixed, treated with 0.05% trypsin for 2 min at 37ºC to remove cell surface protein, permeabilized, and stained with an anti-LepR antibody to visualize intracellular LepR. Left panels show immunofluorescence images depicting intracellular localization of LepR at different time points. The right panel displays a boxplot of fluorescence intensity per cell. Red represents fluorescence intensity at 0 min post-leptin stimulation (n = 34), blue represents fluorescence intensity at 30 min post-leptin stimulation (n = 65), green represents fluorescence intensity at 90 min post-leptin stimulation (n = 172). Scale bar, 40 µm. Statistical significance was determined using one-way analysis of variance (ANOVA) followed by Bonferroni's post-hoc comparison tests. ** $p < 0.01$ between 0 min and 90 min, as well as between 30 min and 90 min.

Figure 3. Immunostaining of intracellular HS and LepR in cells treated with and without HSase. A: Cells were either untreated or treated with HSase for 30 min and then stimulated with leptin. At 0, 15, and 90 min post-stimulation, cells were stained with antibodies to visualize the localization of HS (green) and LepR (red). B: Co-staining of HS with various intracellular markers (Syntaxin6, Clathrin, EEA1, and APPL1). Intracellular markers are shown in red, HS in green, and DAPI in cyan. Arrowheads indicate the co-localization with intracellular markers. C: Co-localization analysis of HS and LepR was performed using ImageJ software. Figure 3C is an enlarged view of the area outlined by a white square in Figure 3A (middle). Areas where HS and LepR colocalize after 15 minutes of leptin treatment are highlighted in white. –HSase denotes cells untreated with HSase; +HSase denotes cells treated with HSase. D: Co-

localization of HS and LepR at the top, middle, and basal regions of the cell. Upper panels show HS is presented in green, and LepR in red. Lower panels display co-localization analysis using ImageJ, with co-localization sites depicted in white. A, C, and D: –HSase denotes cells untreated with HSase; +HSase denotes cells treated with HSase. A-D: Scale bar, 20 μm.

Figure 4. Analysis of heparin interaction with FLAG-LepRΔC using the photoreactive crosslinker SBED-heparin. A: Western blotting of FLAG-tagged proteins from cell lysates transfected with FLAG-CMV14 (negative control vector), FLAG-m6ST3, and FLAG-LepRΔC. B: Cell lysates were incubated with SBED-heparin and subjected to crosslinking. Immunoprecipitation of FLAG-tagged proteins using M2 beads was followed by detection of crosslinked biotin using Alexa594-streptavidin staining. Images depict beads with (+Hep) and without (–Hep) free heparin as a competitor. Scale bar, 500 μm. C: Boxplot showing fluorescence intensity. Results from cell lysates transfected with FLAG-CMV14, FLAG-m6ST3, and FLAG-LepRΔC are presented. Statistical significance was determined using Welch's t-test between –Hep and +Hep for each cell lysate. ***, $p < 0.001$.

Figure 5. Interaction between LepR and Lrp1 in cells treated with HSase and leptin. A: Western blot depicting LepR expression in cells subjected to combined HSase and leptin treatments. Cells were untreated or treated with HSase for 30 min, followed by stimulation with or without leptin for another 30 min. Equal amounts of protein extract (35 μg) were loaded. B: Immunoblot analysis of LepR precipitation using two different antibodies. The amount of LepR in the precipitates was detected. LepR and Ob-R denote the two antibodies used against LepR. C: Western blot showing Lrp1 expression in cells treated with HSase and leptin. Equal amounts of protein extract (35 μg) were loaded. D: Immunoblot analysis of LepR precipitation using two different antibodies after Lrp1 precipitation. The positions of the molecular weight markers are indicated on the left side (A and C) or both sides (B and D) of the figure. E: Top and middle graphs display the amounts of LepR and Lrp1 in the immunoprecipitates, respectively. The

bottom graph presents relative levels of LepR and Lrp1, normalized to a value of 1 for untreated samples. Data represent averaged results from three independent experiments with error bars. Statistical significance was determined between conditions without and with HSase in the presence of leptin, using Student's t-test. ** $p < 0.01$.

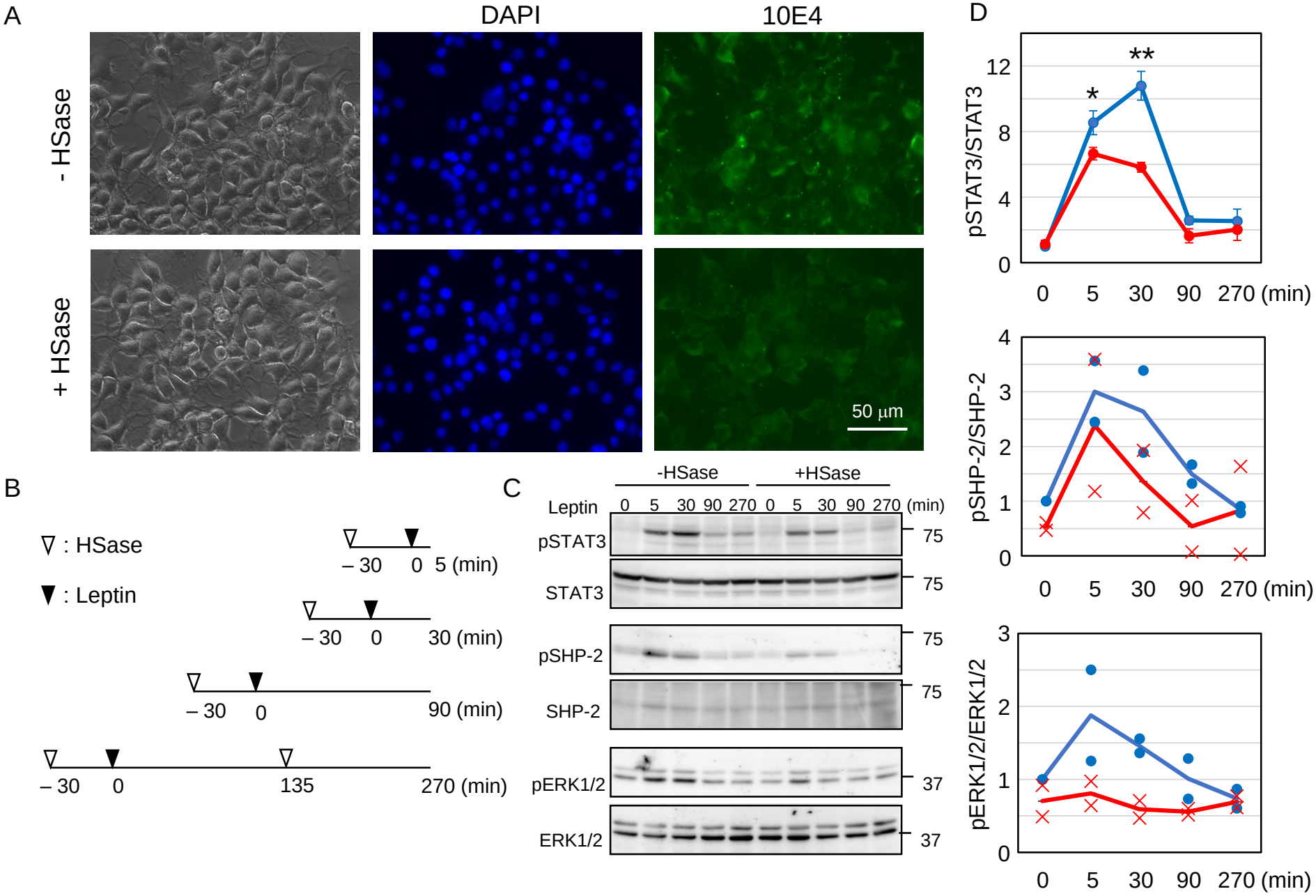

Figure 1

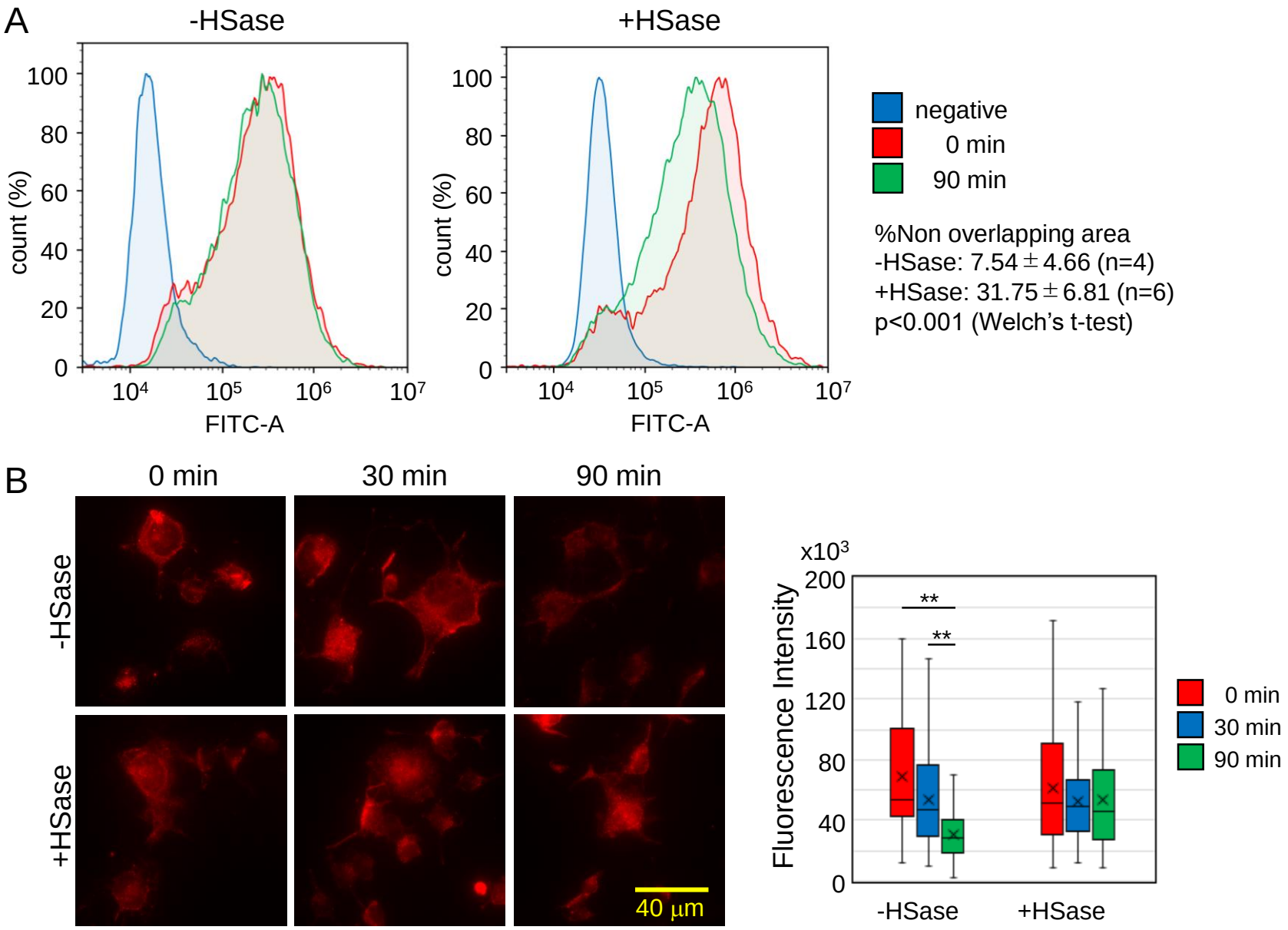
A
-HSase
+HSase
count (%)
FITC-A
negative
0 min
90 min
%Non overlapping area
-HSase: 7.54 ± 4.66 (n=4)
+HSase: 31.75 ± 6.81 (n=6)
p<0.001 (Welch's t-test)
B
0 min
30 min
90 min
-HSase
+HSase
40 μm
x10³
Fluorescence Intensity
**
**
0 min
30 min
90 min

Figure 2

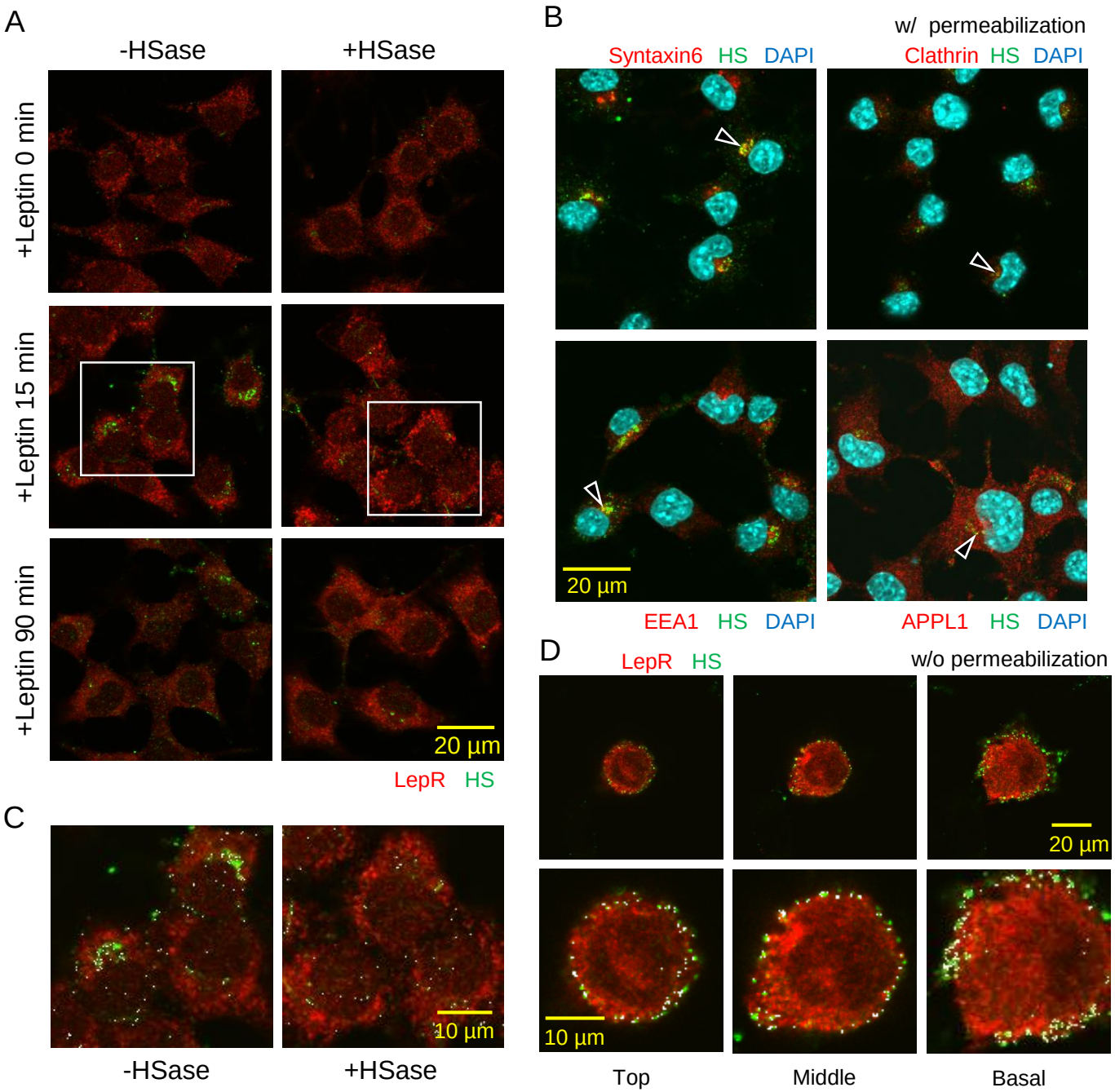
A
-HSase
+HSase
+Leptin 0 min
+Leptin 15 min
+Leptin 90 min
20 μm
LepR HS
B
w/ permeabilization
Syntaxin6 HS DAPI
Clathrin HS DAPI
20 μm
EEA1 HS DAPI
APPL1 HS DAPI
C
10 μm
-HSase
+HSase
D
LepR HS
w/o permeabilization
20 μm
10 μm
Top
Middle
Basal

Figure 3

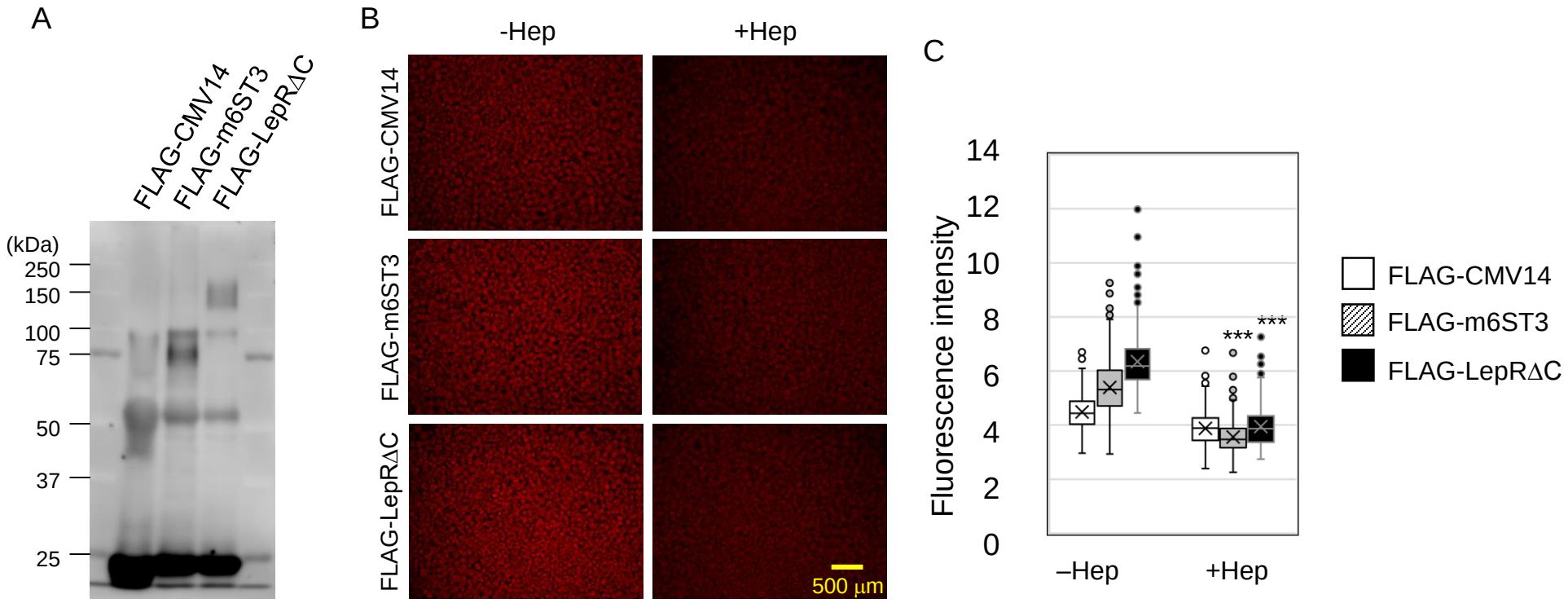
A
FLAG-CMV14
FLAG-m6ST3
FLAG-LepRΔC
(kDa)
250
150
100
75
50
37
25
B
-Hep
+Hep
FLAG-CMV14
FLAG-m6ST3
FLAG-LepRΔC
500 μm
C
Fluorescence intensity
14
12
10
8
6
4
2
0
***
***
–Hep
+Hep
FLAG-CMV14
FLAG-m6ST3
FLAG-LepRΔC

Figure 4

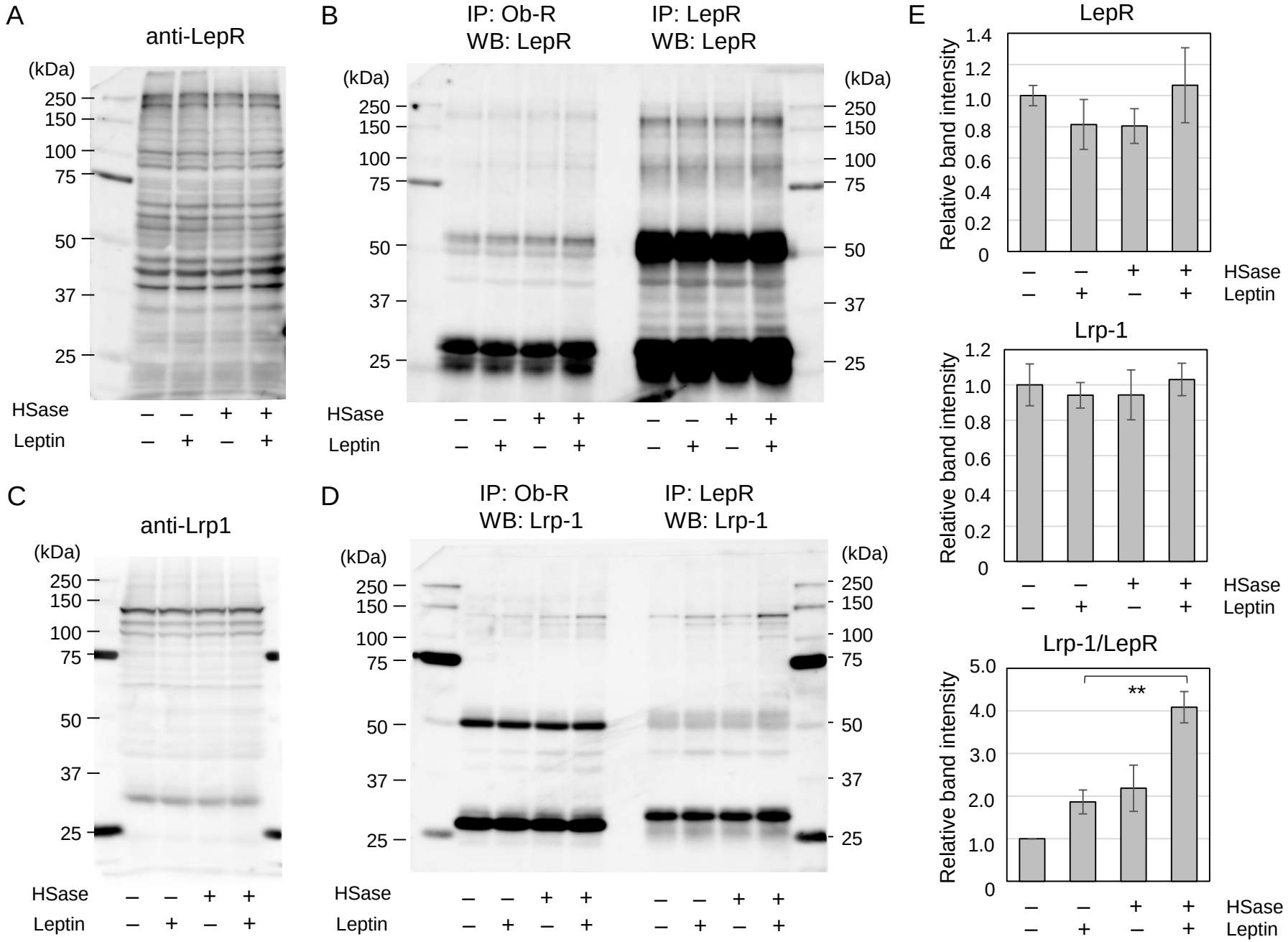
A
anti-LepR
(kDa)
250
150
100
75
50
37
25
HSase
Leptin
B
IP: Ob-R
WB: LepR
IP: LepR
WB: LepR
C
anti-Lrp1
D
IP: Ob-R
WB: Lrp-1
IP: LepR
WB: Lrp-1
E
LepR
Lrp-1
Lrp-1/LepR
Relative band intensity
**

Figure 5

Supplementary Materials and Methods

Analysis of HS disaccharide composition. Cells cultured in 6 cm dishes (CS) or 10 cm dishes (HS) at confluency were used for analysis. The cells were treated with 0.2 M NaOH solution overnight at room temperature. After neutralization with 4 M acetic acid, the solution was incubated with 100 μg/mL DNase I and 100 μg/mL RNase A at 37°C for 2 hours. Phenol/CIAA extraction was performed twice, and the supernatant was processed for ethanol precipitation by adding three volumes of cold ethanol containing 1.3% (w/v) potassium acetate. After incubation overnight at -20°C, the glycosaminoglycans were precipitated by centrifugation at 12,000 g for 30 minutes at 4°C. The precipitates were washed once with 70% ethanol and dissolved in water. For CS, the samples were digested with 10 mU Chondroitinase ABC at 37°C for 1 hour. For HS, the samples were analyzed under the same conditions as previously described. The disaccharide compositions of HS were analyzed according to the method described in the previous paper (41).

Genome editing. The 5' and 3' gRNA sequences for *Ext1* are 5'-GAAGAAAGGGCGCAGAGCGTC-3' and 5'-GACGCTCTGCGCCCTTTCTTC-3', respectively. These gRNA sequences were cloned into the pX459 vector obtained from Addgene. Neuro2A-ObRb cells were seeded in a 6-well plate at a density of 2 x 10^5 cells per well, and transfection was performed when the cells reached 70-80% confluency. The vector was mixed with Lipofectamine 3000 according to the manufacturer's protocol and then added to the cells. After 48 hours, puromycin was added to the culture medium at a concentration of 2 μg/mL. Following a 4-day selection period, viable cells were pooled and expanded for further experiments.

Quantitative RT-PCR. Total RNA was extracted from cells transfected with siRNA using the RNeasy Plus Mini Kit (QIAGEN). Reverse transcription was performed with 1 μg of each RNA sample using the ReverTra Ace® qPCR RT Master Mix (TOYOBO) according to the manufacturer's instructions.

Quantitative PCR was then conducted using iTaq Universal SYBR Green Supermix (Bio-Rad) and the QuantStudio® 3 Real-Time PCR System (Applied Biosystems), following the protocols provided by the manufacturers. The primers used for qRT-PCR were as follows: 36B4 forward, 5'-CGACCTGGAAGTCCAACTAC-3'; 36B4 reverse, 5'-ATCTGCTGCATCTGCTTG-3'; Lrp1 forward 5'-GGACCACCATCGTGGAAA-3'; Lrp1 reverse 5'-TCCCAGCCACGGTGATAG-3'.

Flow Cytometry (FACS). Cells were harvested using Accutase (Nacalai Tesque) and washed twice with PBS. To minimize non-specific binding, they were incubated with 1% BSA for 1 h at 4°C. The cells were then stained with either mouse monoclonal anti-HS antibody 10E4 or rabbit polyclonal anti-LepR antibody (961-R, BIOSS) for 1 h at 4°C. After washing twice with PBS, Alexa 488-conjugated secondary antibodies were applied for 1 h at 4°C. Following three additional PBS washes to remove unbound antibodies, the cells were resuspended in PBS and analyzed using a NovoCyte flow cytometer (Agilent).

A

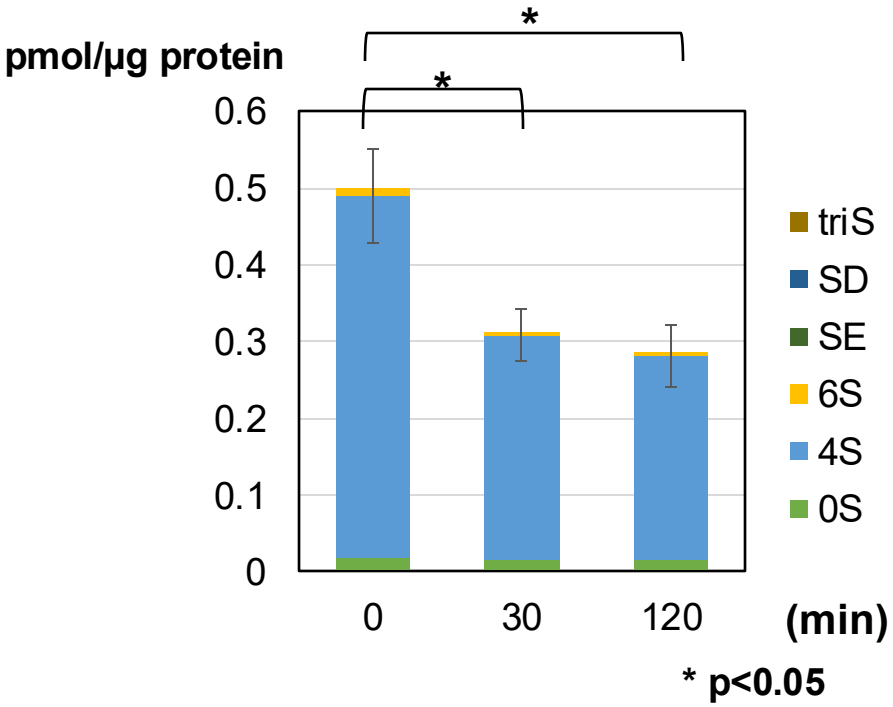

B

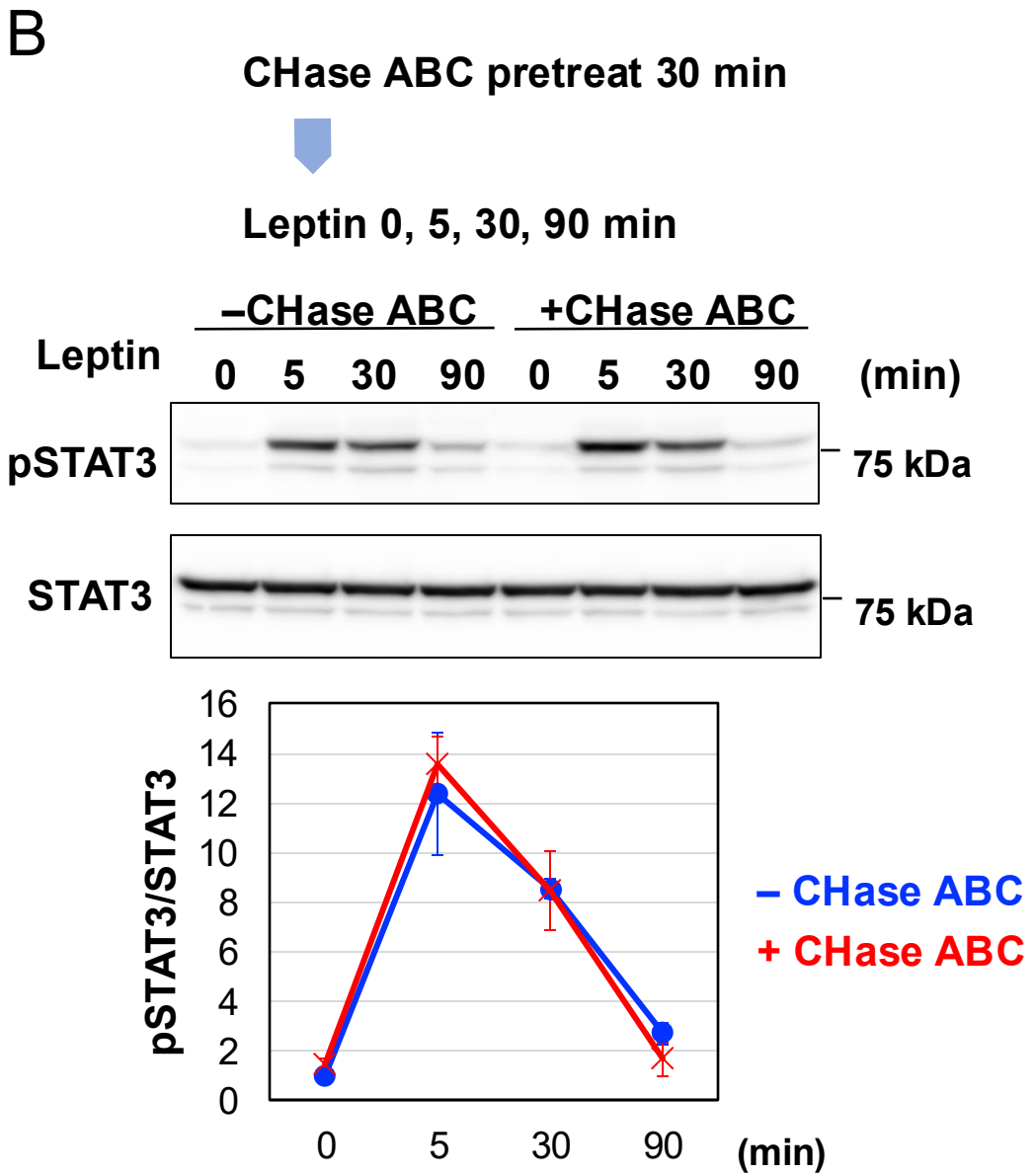

Supplementary Figure 1

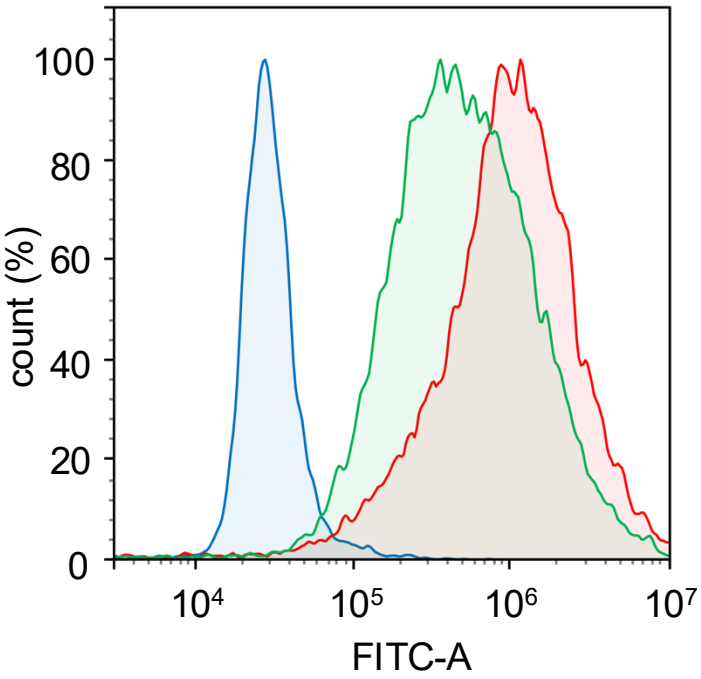

Supplementary Figure 2

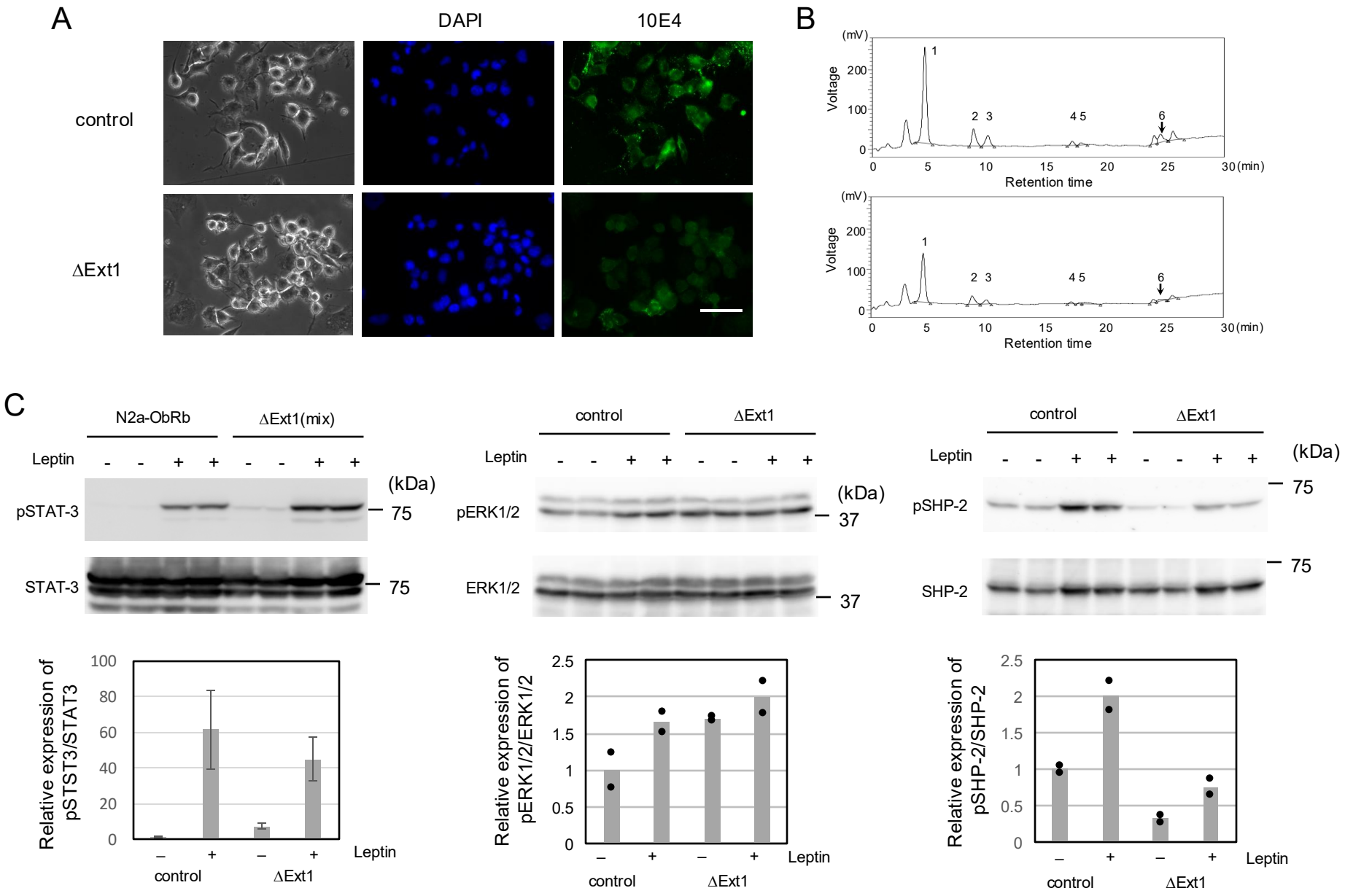

Supplementary Figure 3

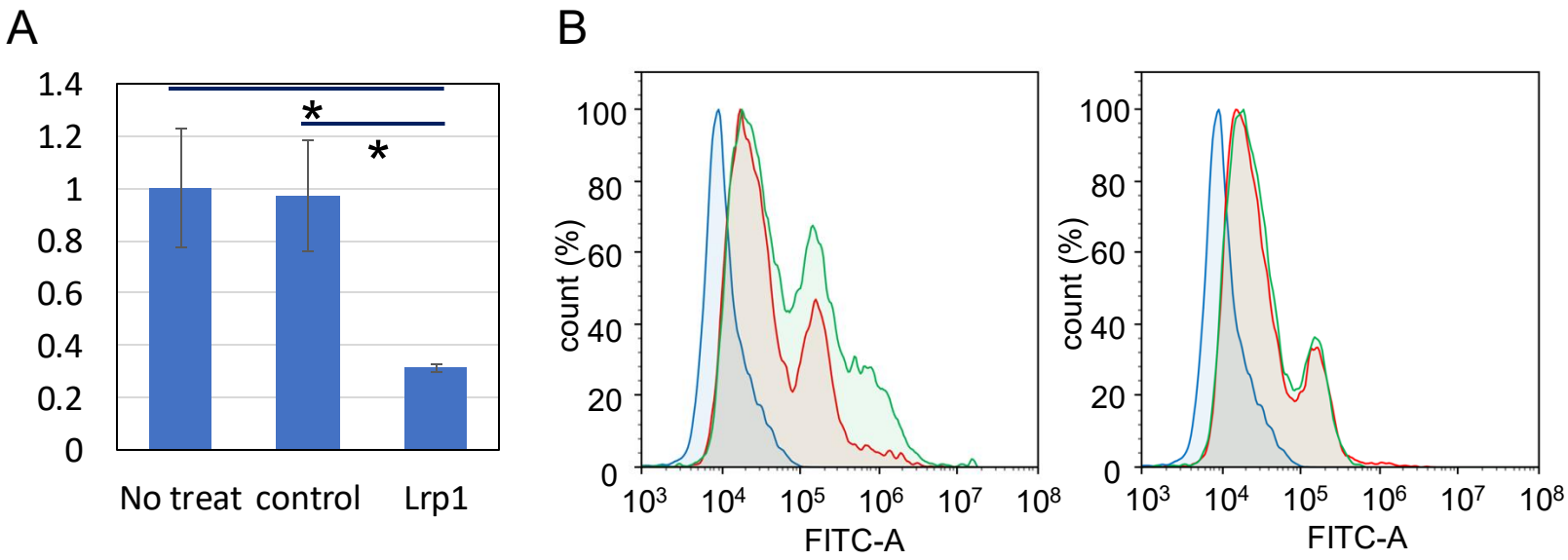

Supplementary Figure 4

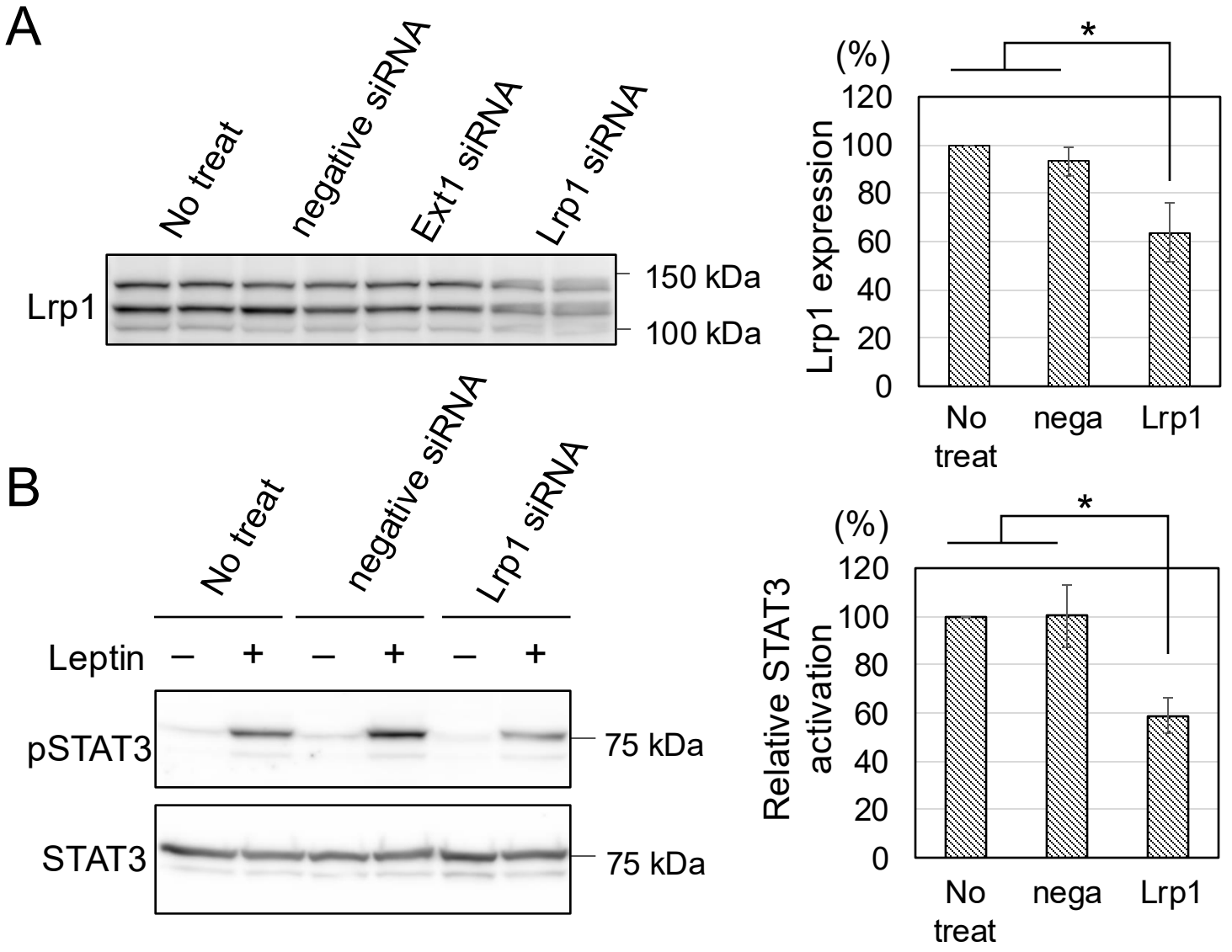

Supplementary Figure 5

Figure legend

Supplementary Figure 1. Impact of CS depletion on leptin signaling in N2A-ObRb cells. A: GAGs were extracted from CHase ABC-treated (+) and untreated (-) N2A-ObRb cells and digested with CHase ABC for disaccharide analysis. The results are shown in the bar graph. The 0S, 4S, 6S, SD, SE and triS shown on the right side of the graph indicates the CS disaccharide unit ΔUA-GalNAc, ΔUA-GalNAc4S, ΔUA-GalNAc6S, ΔUA2S-GalNAc6S, ΔUA-GalNAc4S6S and ΔUA2S-GalNAc4S6S, respectively. CS was reduced by about half in CHase ABC-treated cells. B: Activation status of STAT3 in response to leptin stimulation in both untreated (–CHase ABC) and CHase ABC-treated (+CHase ABC) cells. Cells were either untreated or treated with CHase ABC 30 min before leptin stimulation. Immunoblotting was performed to detect pSTAT3, total STAT3 (STAT3). Equal amounts of protein extract (20 μg) were used. Molecular weight markers are shown on the right side of the panels. Time course of phosphoprotein/total protein is presented as a line graph, normalized to a value of 1 for samples without CHase ABC treatment at t = 0. Data represent the averaged results of three independent experiments with error bars. Blue and red lines indicate the results for –CHase ABC and +CHase ABC, respectively. Bars represent the mean ± S.E.M. Statistical significance was determined using Student's t-test between –CHase ABC and +CHase ABC.

Supplementary Figure 2. The decrease in cell surface HS was confirmed by FACS analysis. Flow cytometry analysis of cell surface HS expression in cells treated with and without HSase. Cells were either untreated (red) or treated with HSase (green). They were then stained with an 10E4 antibody to assess cell surface expression.

Supplementary Figure 3. Impact of knockdown of *Ext1* on leptin signaling in N2A-ObRb cells. A: N2A-ObRb cells (control) and cells with *Ext1* knocked out by genome editing (ΔExt1) were stained with

10E4 antibody to visualize HS (green). Panels show phase-contrast (left), DAPI staining (middle), and 10E4 staining (right). Scale bar, 50 μm. B: Chromatograms of HS disaccharide analysis performed with GAGs extracted from control and ΔExt1 cells. The peaks from 1 to 6 indicate the HS disaccharide unit ΔUA-GlcNAc, ΔUA-GlcNS, ΔUA-GlcNAc6S, ΔUA-GlcNS6S, ΔUA2S-GlcNS and ΔUA2S-GlcNS6S, respectively. HS was reduced by about half in ΔExt1 cells. C: Activation status of STAT3, ERK1/2 and SHP-2 in response to leptin stimulation in both control and ΔExt1cells. (Upper panels) Cells were treated with leptin for 30 min, and immunoblotting was performed to detect pSTAT3, total STAT3 (STAT3), pERK1/2, ERK1/2, pSHP-2 and SHP-2. Molecular weight markers are shown on the right side of the panels. (Lower panels) Time course of phosphoprotein/total protein is presented as a bar graph, normalized to a value of 1 for control cells without leptin treatment. For STAT3, data represent the averaged results (n = 4) with error bars, while data for ERK and SHP-2 represent results f of n=2, with each measurement indicated by circles. Bars represent the mean ± S.E.M. For STAT3, the Mann-Whitney U test showed a significance level of $p<0.05$ for all combinations except the control with leptin addition versus ΔExt1 with leptin addition.

Supplementary Figure 4. A: The bar graph shows the relative expression levels of *Lrp1* in Neuro2A-ObRb cells, Neuro2A-ObRb cells transfected with negative control siRNA, and Neuro2A-ObRb cells transfected with *Lrp1* siRNA. The expression levels were normalized to *36B4* and are presented as fold change relative to untransfected cells. Data are shown as mean ± SD from three independent experiments. Statistical significance was determined using one-way ANOVA followed by the Mann-Whitney U test. *$P < 0.05$. B: The histograms depict the cell surface expression levels of LepR in Neuro2A-ObRb cells treated with *Lrp1* siRNA. Cells without leptin treatment are shown in red, and cells treated with leptin for 30 minutes are shown in green. Blue represents cells stained with normal serum as a negative control. The x-axis represents fluorescence intensity, indicating the level of LepR expression, and the y-axis represents

the relative number of cells, with the highest peak set to 100%. Data are representative of two independent experiments.

Supplementary Figure 5. A: (Left) The Western blot shows the expression levels of Lrp1 in Neuro2A-ObRb cells without transfection, Neuro2A-ObRb cells transfected with negative control siRNA, and Neuro2A-ObRb cells transfected with *Lrp1* siRNA. Data are representative of three independent experiments. (Right) The relative expression levels were quantified by densitometry and normalized. B: (Left) The Western blot shows the activation status of STAT3 in response to leptin stimulation in Neuro2A-ObRb cells without transfection, transfected with negative control siRNA, or with *Lrp1* siRNA. Molecular weight markers are shown on the right side of the panels. (Right) The relative expression of pSTAT3/total STAT3 is presented as a bar graph, normalized to a value of 1 for Neuro2A-ObRb cells without transfection. Data are representative of three independent experiments. Bars represent the mean ± S.E.M. Statistical significance was determined using one-way ANOVA followed by Tukey's t-test. *P < 0.05. Nega, negative control siRNA transfected cells; Lrp1, *Lrp1* siRNA transfected cells.